

Apparatus for positron emission tomography

Marko Starič¹, Samo Korpar¹, Erik Margan¹, Marko Šifrar¹, Aleš Stanovnik^{1,2},
Nataša Budihna³, Metka Milčinski⁴, Boris Šket⁵

¹Jozef Stefan Institute, ²Faculty of Electrical Engineering, University of Ljubljana,

³Institute of Oncology Ljubljana, ⁴Nuclear Medicine Department, Medical Center Ljubljana,

⁵Faculty of Chemistry and Chemical Technology, University of Ljubljana, Slovenia

We describe the upgrade and the performance of a second-hand apparatus for positron emission tomography (PET), at present the only existing PET system in Slovenia. A novel readout system has been designed and assembled with electronic modules obtained from the particle physics laboratory at the Jozef Stefan Institute. The entire system, including the computer programs for data acquisition and image reconstruction, has been tested with point sources, phantoms and on guinea pigs. Results of these tests should permit an evaluation of the clinical potentials of the apparatus.

Key words: tomography, emission-computed

Introduction

Positron emission tomography (PET) measures the spatial distribution of an organic substance, which has been labeled with a positron emitting isotope. The positron emitted by the isotope is stopped within about a millimeter from the parent nucleus, where it is annihilated with an electron in the tissue, giving rise to two back-to-back, 511 keV photons. An advantage of this method over single photon emission computed tomography (SPECT) is that it requires no collimators as the gamma ray direction is determined by the positions of the two coincidental hits. Fur-

thermore, positron emitting isotopes of elements composing organic molecules have suitable lifetimes (e.g. ¹¹C, ¹³N, ¹⁵O). Especially interesting is the labeling of glucose with ¹⁸F (FDG, fluoro-deoxy-glucose) for measurements of metabolism in human tissue.

For some time researchers at the Jozef Stefan Institute have been interested in the development of an apparatus for positron emission tomography based on multiwire proportional chambers. With a small test apparatus, they have demonstrated a resolution of 3 mm full width at half maximum (FWHM) on the reconstructed three dimensional (3D) image of a point source.¹ Given the possibility of ¹⁸F production through neutron activation of an isotopically enriched Li₂CO₃ target at the TRIGA reactor of the

Correspondence to: Prof. Dr. Aleš Stanovnik, dipl. ing., Faculty of Electrical Engineering, University of Ljubljana, Tržaška 25, 1000 Ljubljana, Slovenia. Fax: +386 61 125 7074 or +386 61 219 385.

Jozef Stefan Institute² and the know-how for synthesis of fluorodeoxyglucose (FDG) at the Faculty of Chemistry and Chemical Technology of the University of Ljubljana³ a full PET system would be desired. The authors of the present paper were thus very pleased and are thankful to the University Clinic of Hannover for the kind donation of their older PET apparatus. At present this is the only PET system in Slovenia so we believe that it is of interest to describe our work on the upgrade of the apparatus as well as to present the results of measurements of some parameters which are indicative of the performance of the system.

Apparatus

The model 4200 PET apparatus, produced by the Cyclotron Corporation, is shown in Figure 1. It has two measuring heads that may

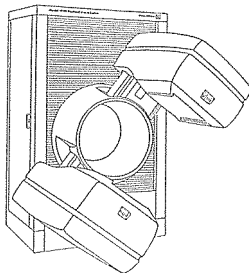


Figure 1. PET apparatus model 4200 produced by Cyclotron Corporation.

rotate around the object in which the activity distribution is to be measured. Besides rotations, tangential and radial displacements of each head separately are also possible. The measuring head consists of 140 sodium iodide (NaI) crystals (ϕ 20 mm, $d=38$ mm), each one viewed by two of the 81 photomultipliers (RCA 6199) as shown in Figure 2. The existing readout system was quite complicated and slow due to the limited data transfer rate and memory space of the old PDP-11 computer.

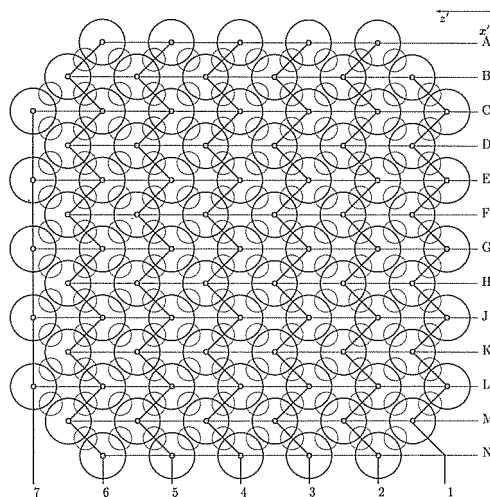


Figure 2. Arrangement of NaI scintillators (small circles) and photomultipliers (larger circles) in a measuring head. The photomultiplier signals are connected into 13 rows (A to N) and 7 zigzag columns (1 to 7).

Given the larger capacity and higher speed of modern computers, a new readout system was designed and manufactured.

After preamplification, the signals from the photomultipliers are connected in rows and columns as indicated in Figure 2. A scintillation in a crystal will thus give rise to pulses in two adjacent rows and either in one column or in two adjacent columns, which uniquely specify the position of the crystal that was hit. The pulses on the rows and columns were led to two specially designed 20-channel pulse shaping modules,⁴ one module for each measuring head (Figure 3). The 270 ns long, shaped pulses were then led to 16-channel input-output CAMAC registers (CAEN C219), from where the information was read into computer memory, subject to the simultaneous presence of a strobe pulse. The strobe signal was generated by the time coincidence (EG&G CO4010) of at least one pulse on each measuring head. The width of the OR pulses for this coincidence was 20 ns.

The output voltage from a potentiometer, which turns under rotations of the measuring heads, indicates the angular position. Simi-

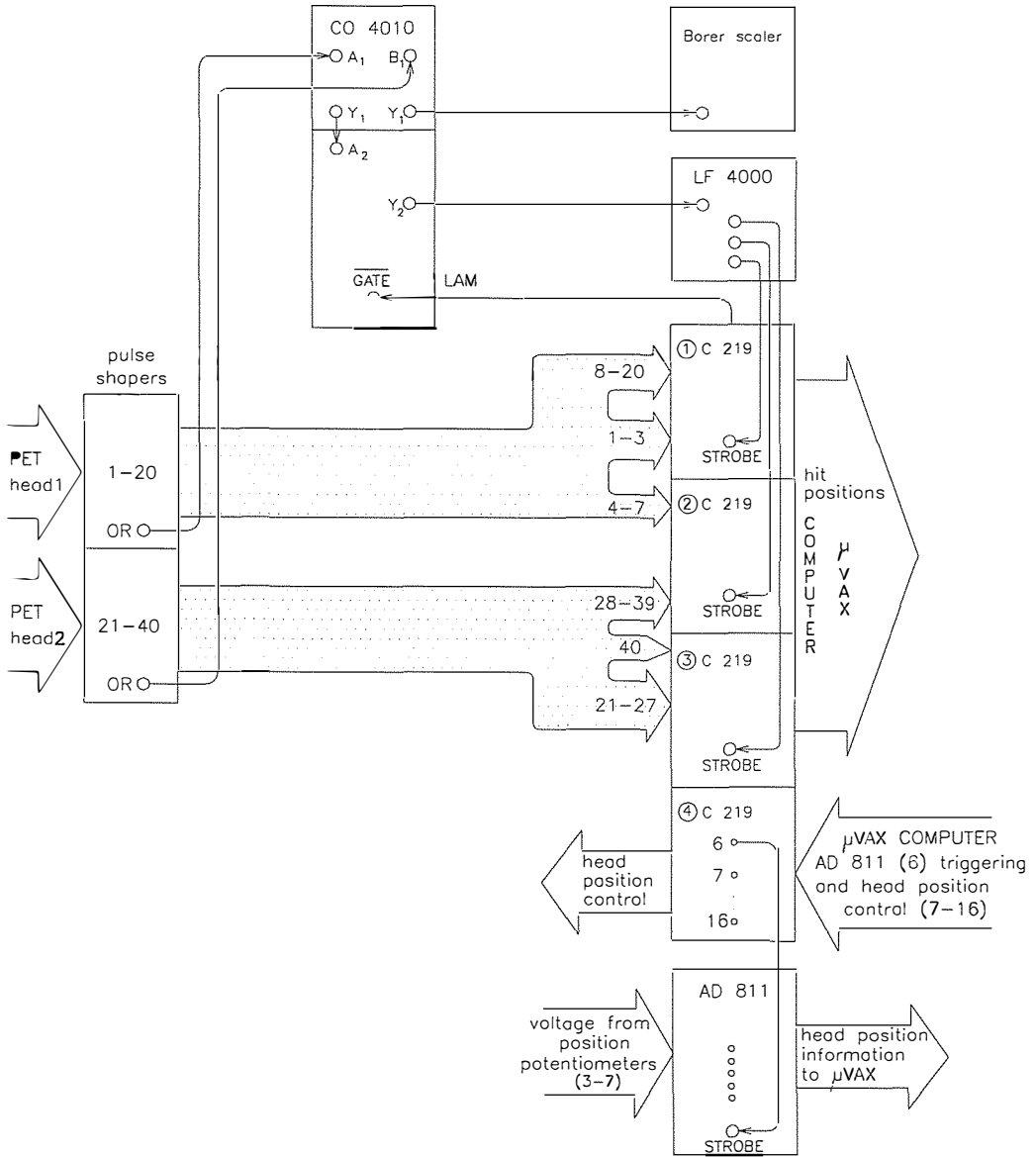


Figure 3. Block diagram of readout electronics. Signals from the measuring heads arrive to pulse shapers on the left-hand side of the diagram and are transferred via CAMAC I/O registers (C219 modules) to the μ VAX computer on the right-hand side of the diagram.

larly, two potentiometers on each head respond to radial and tangential displacements. The output voltages of all these potentiometers have been calibrated against corre-

sponding positions of the measuring heads.⁵ The voltage levels are converted to digital form in the 8-channel analog-to-digital converter (EG&G AD-811), which can be read

into the computer when required. The request is given by the computer through an input-output CAMAC register (CAEN C219) in the form of a strobe signal for the ADC. By means of this same I/O register, signals can also be sent by the computer to switches that control motors for displacing the measuring heads (Figure 3).

The computer programs for data acquisition⁵ and for 3D image reconstruction⁶ have been written and optimized for the specific apparatus described above and represent a substantial part of the work done in order to improve the performance of the system.

Performance of the system

The system performance was tested with a ^{22}Na point source, with two distributions of H^{18}F solutions - the so called phantoms, and with a small test animal.

Efficiency

The ^{22}Na positron point source of 0.35 MBq activity is embedded in a 4 mm thick plastic disk covered with Al plates in which the positrons annihilate into pairs of 511 keV photons. With the point source on the axis at a distance of 84 cm from the measuring head, the numbers of hits on each individual NaI crystal were measured. These numbers are roughly proportional to the efficiency of each crystal and are shown in Figure 4. The average efficiency of the crystals, defined as the number of counts divided by the number of incident 511 keV photons, has been measured in a separate experiment relative to a larger NaI counter (ϕ 50 mm, $d=50$ mm) and found to be approximately 45% with a voltage of 1350 V on the photomultipliers. As only 40% of the surface of the measuring head (33 cm \times 33 cm) is covered by NaI crystals, we find an overall efficiency of one measuring head to be about 18%.

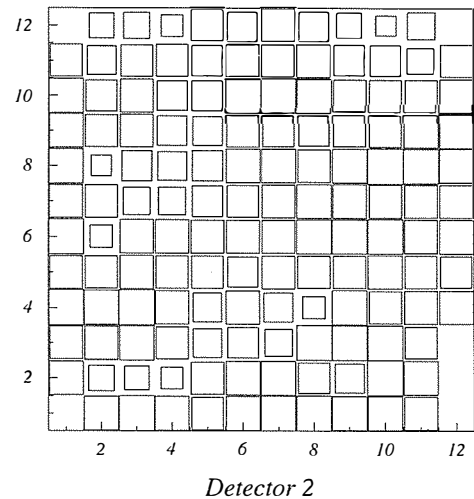
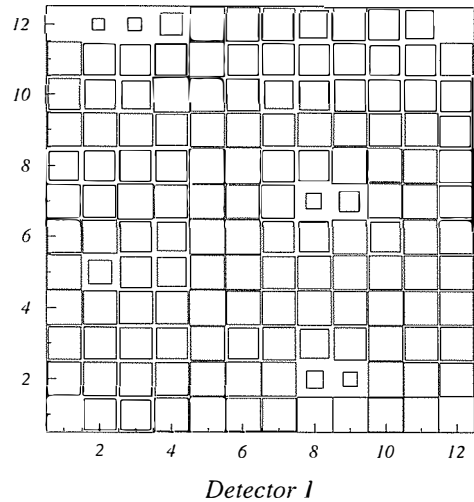


Figure 4. The numbers of hits on individual scintillators, when the measuring head is illuminated by a distant (84 cm) point source, are represented by the surfaces of the squares corresponding to the scintillators.

Position resolution

The point source was then placed in the center of the system and a tomographic image was recorded. After image reconstruction, the profiles through the 3D distribution in three perpendicular directions have been obtained, as shown in Figure 5. The resolution, defined as the full width at half maximum ($\text{FWHM} = 2.35 \times \sigma$) of the distribution,

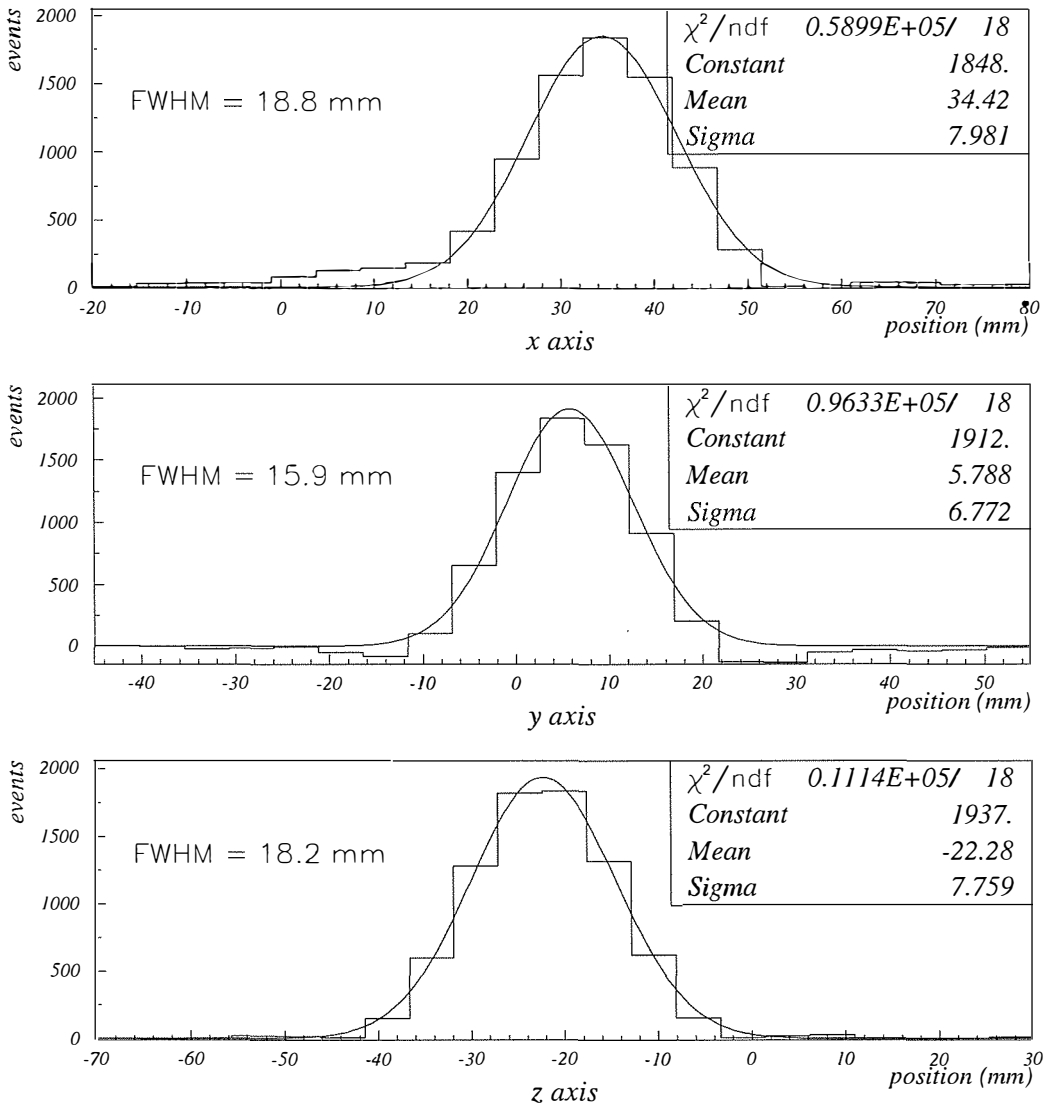


Figure 5. Reconstruction of events measured with a ^{22}Na positron point source, produces distributions in three perpendicular directions (x, y and z) which are fitted with Gaussian functions. The resolution, defined as the full width at half maximum ($\text{FWHM} = 2.35 \times \sigma$), is seen to be about 18 mm.

is seen to be about 18 mm. By surrounding the positron point source with 10 cm of perspex to simulate Compton scattering of the annihilation photons in the human head, no deterioration of the resolution could be observed. Figure 6 shows a slice through the 3D distribution of two point sources at a spacing of 40 mm in air.

Sensitivity

The sensitivity, defined as the coincidence count rate divided by the source activity, was measured to be $2500\text{s}^{-1}/\text{MBq}$ and $900\text{s}^{-1}/\text{MBq}$ for the ^{22}Na point source in air and in the center of a $R=10$ cm perspex sphere, respectively. Besides reducing the absolute coinci-

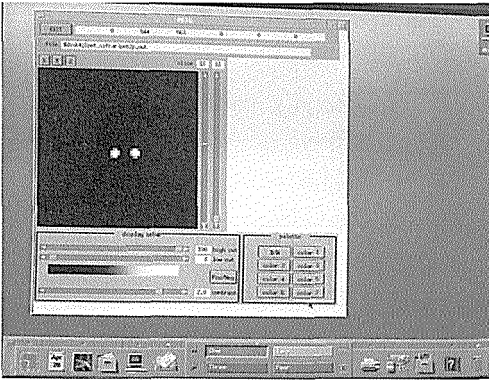


Figure 6. Display of a slice on a CRT computer screen, through the reconstructed 3D image of two point sources at a separation of 40 mm.

dence count rate, Compton scattering is also responsible that about 2/3 of this reduced rate actually represents background events, which deteriorate the image contrast. The singles count rate of each measuring head was about $25 \cdot 10^3 \text{ s}^{-1}$, resulting in a random coincidence rate of only 25 s^{-1} , which does not contribute significantly to the sensitivity numbers discussed above.

Phantoms

The standard phantom, a cylinder with 22.3 cm diameter and 18.5 cm high, is divided into an upper and a lower part. The upper part contains six spheres of different sizes ($2R=32, 25, 19, 16, 13$ and 10 mm) at the corners of a regular hexagon with 58 mm sides. The spheres are held by thin plastic rods, which are fixed to the bottom of the container. The lower half is divided into six sectors, each one filled with equally-spaced plastic rods of different number and size (rod diameters between 5 and 11 mm in steps of 1 mm, rod spacing between 10 and 25 mm in steps of 3 mm, numbers of rods in a sector range from 10 for the large rods to 58 for the smallest ones). The space between the plastic rods and spheres was filled with an initial activity of 20 MBq of H^{18}F , which was dissolved in

water to a specific activity of 3 kBq/cm^3 . The initial individual head count rates, the coincidence and random coincidence rates were $480 \cdot 10^3 \text{ s}^{-1}$, $21 \cdot 10^3 \text{ s}^{-1}$ and $9 \cdot 10^3 \text{ s}^{-1}$ respectively, and the dead time was 20%. In 2.5 hours about 48 million coincident events were measured. The reconstruction required 10 hours of the $\mu\text{VAX IV}$ computer resulting in a 3D distribution through which two slices are

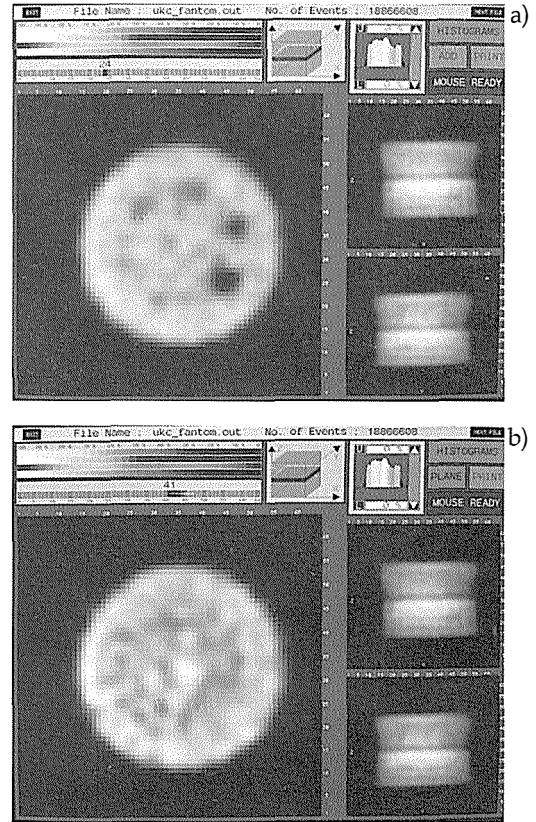


Figure 7. Distribution of activity in two slices through the reconstructed 3D image of the standard phantom. a) The slice is through the plastic spheres imbedded in 3 kBq/cm^3 of H^{18}F solution. b) The slice is through the plastic rods arranged by diameter and spacing into six sectors in the lower part of the phantom. The position resolution of 18 mm FWHM does not allow the individual rods to be resolved.

shown in Figure 7. It is seen that the rods are not resolved well, which should be expected as the largest rods have diameters less than

two thirds of the 18 mm FWHM resolution. Four of the largest spheres, on the other hand, are clearly observed while the smallest two can possibly be seen by an experienced eye only.

Measurement of a different distribution of HF labeled with ^{18}F was also performed. A small bottle with 50 ml of 40 kBq/cm^3 solution was fixed inside a 450 ml plastic bottle (truncated 1.5 liter bottle for Radenska mineral water), which was filled with 10 kBq/cm^3 of solution and in turn was put inside a larger 1000 ml plastic bottle (truncated 2 liter Coca Cola bottle) filled with 20 kBq/cm^3 of HF solution. The overall activity was about 18 MBq and the singles, coincidence and random coincidence count rates were $420\ 10^3\ \text{s}^{-1}$, $37\ 10^3\ \text{s}^{-1}$ and $7.2\ 10^3\ \text{s}^{-1}$ respectively. In half an hour 11 million events were measured and the distribution shown in Figure 8 was reconstructed.

Guinea pig

In a previous experiment with the measuring heads static and the measured object rotating, we measured a guinea pig injected with a solution of H^{18}F . With an accumulated 10 million events, a 3D distribution was reconstructed, with cross sections as shown in Figure 9. A concentration of activity is seen in the bladder, the lungs and in the head. By comparing distributions measured at different times after the injection, the bladder activity has been observed to increase with time.

Conclusions

We have repaired and upgraded a second-hand apparatus for positron emission tomography, at present the only existing PET apparatus in Slovenia. For the donation we are grateful to professors G. Meyer and H. Hundseshagen from the University of Hannover.

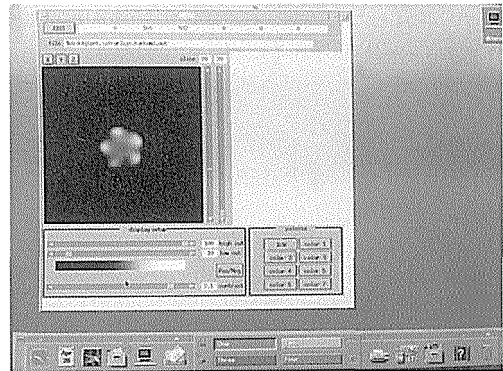


Figure 8. The display of the reconstructed activity distribution in various slices of the phantom manufactured by the authors. a) The absence of activity below the innermost bottle is due to the plastic support for this bottle. b) A slice through the pentagonal bottom of the Coca-Cola bottle.

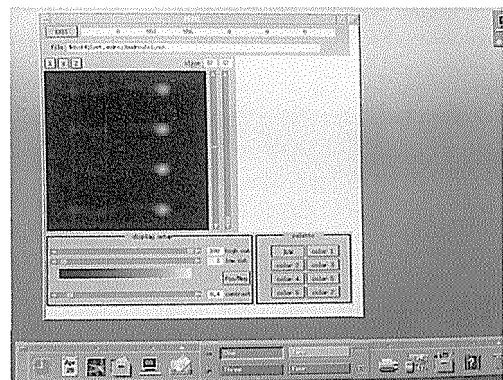


Figure 9. Slices through the reconstructed activity distribution in a guinea pig. Four distributions are shown with time increasing from bottom to top, so the increasing activity of the bladder could be observed.

Although the parameters, notably the position resolution of about 18 mm FWHM, are not at the level of modern commercial devices, it should nevertheless be worth considering our apparatus as a training system on which research could be done and know-how could be obtained in order to facilitate and secure proper use of a new system when such a system is purchased.

We are planning to perform some further measurements with FDG on test animals in order to evaluate the possibility of doing some clinical measurements of larger human organs such as for example the liver or the lungs.

References

1. Starič M, Korbar D, Stanovnik A. Tests of a mini positron emission tomograph based on multiwire proportional chamber. *Physica Medica* 1993; **9**: 219-23.
2. Fajgelj A, Novak J, Stegnar P, Dimic V, Kužnik A. Preparation of ^{18}F -fluorid for labeling organic compounds using a low-power research reactor. *Vestnik Slov Kem Društva* 1985; **32**: 319-24.
3. Erjavec M, Fajgelj A, Guna F, Novak J, Šket B. Synthesis and clinical experiments with ^{18}F -3-deoxi-glucose. Upsala: 8th International Symposium on Medical Chemistry; 1984. p. 65.
4. Margan E. Design of pulse shapers for PET. Ljubljana: Institute Jožef Štefan; 1996.
5. Šifrar M. *Krmiljenje pomikov in preizkus delovanja scintilacijskega pozitronskega tomografa*. [Diplomsko delo]. Ljubljana: Univerza v Ljubljani; 1996.
6. Korbar D, Stanovnik A, Starič M. Primerjava algoritmov za rekonstrukcijo 3D tomografske slike med direktnim 3D Fourierjevim obratom in rekonstrukcijo preko 2D projekcij. [Report, IJS DP-5183] Ljubljana: Institute Jožef Štefan; 1988.